

Accepted Manuscript

Title: NANOARCHITECTURES BASED ON MULTI-WALLED CARBON NANOTUBES NON-COVALENTLY FUNCTIONALIZED WITH CONCANAVALIN A: A NEW BUILDING-BLOCK WITH SUPRAMOLECULAR RECOGNITION PROPERTIES FOR THE DEVELOPMENT OF ELECTROCHEMICAL BIOSENSORS



Authors: Elvis Ortiz, Pablo Gallay, Laura Galicia, Marcos Eguílaz, Gustavo Rivas

PII: S0925-4005(19)30647-1
DOI: <https://doi.org/10.1016/j.snb.2019.04.114>
Reference: SNB 26483

To appear in: *Sensors and Actuators B*

Received date: 13 March 2019
Revised date: 21 April 2019
Accepted date: 23 April 2019

Please cite this article as: Ortiz E, Gallay P, Galicia L, Eguílaz M, Rivas G, NANOARCHITECTURES BASED ON MULTI-WALLED CARBON NANOTUBES NON-COVALENTLY FUNCTIONALIZED WITH CONCANAVALIN A: A NEW BUILDING-BLOCK WITH SUPRAMOLECULAR RECOGNITION PROPERTIES FOR THE DEVELOPMENT OF ELECTROCHEMICAL BIOSENSORS, *Sensors and Actuators: B. Chemical* (2019), <https://doi.org/10.1016/j.snb.2019.04.114>

This is a PDF file of an unedited manuscript that has been accepted for publication. As a service to our customers we are providing this early version of the manuscript. The manuscript will undergo copyediting, typesetting, and review of the resulting proof before it is published in its final form. Please note that during the production process errors may be discovered which could affect the content, and all legal disclaimers that apply to the journal pertain.

**NANOARCHITECTURES BASED ON MULTI-WALLED CARBON
NANOTUBES NON-COVALENTLY FUNCTIONALIZED WITH
CONCAVALIN A: A NEW BUILDING-BLOCK WITH SUPRAMOLECULAR
RECOGNITION PROPERTIES FOR THE DEVELOPMENT OF
ELECTROCHEMICAL BIOSENSORS**

Elvis Ortiz^{1,2}, Pablo Gallay¹, Laura Galicia^{2,*}, Marcos Eguílaz^{1,*}, Gustavo Rivas^{1,*}

**¹INFIQC. Departamento de Físicoquímica. Facultad de Ciencias Químicas.
Ciudad Universitaria. 5000 Córdoba. Argentina.**

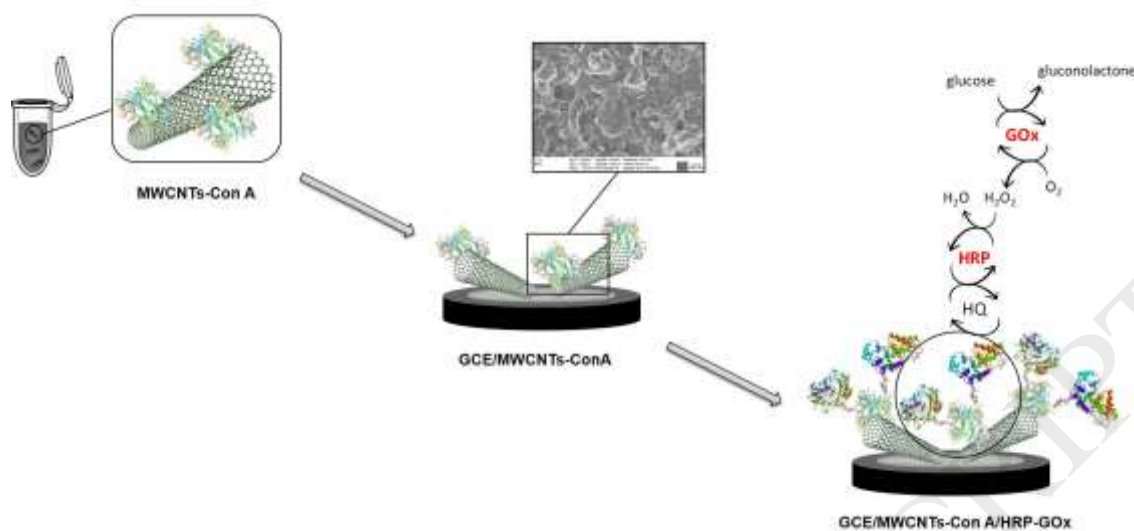
**²Departamento de Química. Universidad Autónoma Metropolitana
Iztapalapa. Av. Michoacán y la Purísima, Col. Vicentina.
C.P. 09340, México.**

***Corresponding author**

e-mail: grivas@fcq.unc.edu.ar; mrubio@fcq.unc.edu.ar

Phone number: +54-351-5353866; Fax number: +54-351-4334188.

Graphical abstract



Highlights

- ConA successfully disperses MWCNTs and gives to them biorecognition properties
- ConA maintains the recognition properties after the drastic dispersing conditions
- GCE/MWCNTs-ConA is a versatile platform to immobilize glycobiomolecules
- HRP and GOx were attached to GCE/MWCNTs-ConA as proof-of-concept
- GCE/MWCNT-ConA/HRP-GOx allowed the highly sensitive/selective quantification of glucose
- GCE/MWCNT-ConA/HRP-GOx was successfully used for detecting of glucose in complex matrices
- GCE/MWCNT-ConA/HRP-GOx was successfully used to quantify glucose in human serum

ABSTRACT

We propose an innovative nanoarchitecture for the development of electrochemical biosensors based on the non-covalent functionalization of multi-walled carbon nanotubes (MWCNTs) with the lectin Concanavalin A (ConA) and

the site-specific supramolecular binding of glyco-biomolecules. As proof-of-concept, we propose the use of two glycoenzymes, glucose oxidase (GOx) and horseradish peroxidase (HRP), for building mono- and bienzymatic glucose biosensors. The selected conditions for the preparation of the dispersion were 1.5 mg MWCNTs in 1.0 mL of 2.0 mg mL⁻¹ ConA sonicated for 5.0 min with sonicator probe. The monoenzymatic glucose biosensor was prepared by casting GCE with the MWCNTs-ConA dispersion (GCE/MWCNTs-ConA) followed by the interaction with GOx (GCE/MWCNTs-ConA/GOx), while the bienzymatic one was obtained by interaction of GCE/MWCNTs-ConA with GOx + HRP (GCE/MWCNTs-ConA/GOx-HRP). The best analytical performance was obtained with the bienzymatic biosensor from the amperometric response at -0.050 V in the presence of 1.0 x 10⁻⁴ M hydroquinone. The sensitivity was (2.22 ± 0.03) μA mM⁻¹ (which was 5.2 times higher than the one obtained with the monoenzymatic biosensor) and a detection limit of 0.31 μM. The reproducibility was 5.4 % and the biosensor was challenged with human blood serum showing an excellent correlation with the values reported by the laboratory.

Keywords: Multi-walled carbon nanotubes functionalization; Concanavalin A; Glucose electrochemical biosensor; Bienzymatic biosensor; Site-specific supramolecular binding.

1. INTRODUCTION

The search for novel bioanalytical platforms able to conjugate an efficient immobilization of biomolecules with an improved electroanalytical performance in terms of sensitivity and selectivity, is a transcendental challenge in the field of

advanced electrochemical biosensors [1,2]. In this context, carbon nanotubes (CNTs) have proven to be an excellent material for the development of innovative electrochemical biosensors due to their unique electronic, physical and chemical properties [3,4]. However, one of the major problems of using CNTs for the preparation of electrochemical (bio)sensors is their strong tendency to form agglomerates due to strong van der Waals and π - π interactions [5]. In this regard, the non-covalent functionalization of CNTs has received considerable attention to minimize these interactions and improve their compatibility with the solvent without disturbing their π -conjugated structure [6–9]. Moreover, the rational selection of the functionalizing agent represents a very promising strategy to prepare tailor-made design of CNTs with specific properties [10].

The oriented and site-specific immobilization of enzymes is essential for the rational design of biosensors, avoiding difficulties related to the random immobilization of enzymes that would produce substantial loss of activity due to structural deformation and shielding of the active binding sites [11,12]. Lectins represent interesting and attractive molecular recognition elements for the oriented immobilization of glycoproteins through sugar-lectin biospecific interactions [13–16]. In particular, Concanavalin A (ConA) is a homotetramer protein (molecular weight, 104 kDa for tetramer) that contains four specific sites with sugar recognition properties for supramolecular binding of polysaccharides, glycoproteins and glycolipids through D-glucose and D-mannose residues [17–19]. It is important to remark that the binding of a glycoenzyme through its carbohydrate residues is not likely to affect neither its prosthetic site nor its biocatalytic activity. The carbohydrate region is generally located in areas which

are not involved in the catalytic activity of these enzymes, retaining most of their biological function even when their sugar chains are blocked [20,21].

Several works have reported the functionalization of CNTs with ConA through the use of different linkers attached to the nanostructures; however, to the best of our knowledge, the direct functionalization of CNTs with ConA has not been reported yet. Xue et al. [22] have proposed the attachment of ConA to multi-walled carbon nanotubes (MWCNTs) non-covalently functionalized with poly(diallyl dimethylammonium chloride) by electrostatic interactions. Li et al. [23] have reported the use of MWCNTs modified with Pt nanoparticles and chitosan for further immobilization of Con A through electrostatic interactions. The non-covalent functionalization of SWCNTs with n-dodecyl β -D-maltoside for the immobilization of ConA through the maltoside residues has been reported by Li et al. [24]. Papper et al. [25] have described the synthesis and electropolymerization of a pyrrolic ConA derivative onto a MWCNTs-modified electrode.

In this work, we propose a new strategy to non-covalently functionalize MWCNTs with ConA in a direct way and to provide them of specific properties for the supramolecular immobilization of glycoenzymes. In the following sections we discuss the preparation, optimization and characterization of MWCNTs-ConA dispersion, and the analytical application of GCE modified with this dispersion for the preparation of monoenzymatic (GCE/MWCNTs-ConA/GOx) and bienzymatic (GCE/MWCNTs-ConA/HRP-GOx) glucose biosensors through the supramolecular immobilization of GOx and GOx + HRP, respectively.

2. EXPERIMENTAL

2.1. Chemicals and solutions

Multi-walled carbon nanotubes (MWCNTs, (30 ± 15) nm diameter, (1-5) μm length and purity higher than 95%), were supplied from Nanolab (USA). Concanavalin A (ConA) (Type VI, from *Canavalia ensiformis*), glucose oxidase (GOx) (Type X-S, from *Aspergillus niger*, EC 1.1.3.4, 157,500 units/g of solid), horseradish peroxidase (HRP) (Type I, 120 units/mg of solid), uric acid and hydroquinone were purchased from Sigma. β -D-(+)-glucose was obtained from Merck. Hydrogen peroxide (30% v/v aqueous solution), ascorbic acid, NaH_2PO_4 and Na_2HPO_4 were supplied from Baker. Other chemicals were of analytical grade and used without further purification. The analyzed samples were nasal spray Alenys[®] (purchased from a local drugstore) and Standatrol SE serum (obtained from Wiener lab.)

A 0.050 M phosphate buffer solution pH 7.40 was employed as supporting electrolyte. Ultrapure water ($\rho = 18.2 \text{ M}\Omega \text{ cm}$) from a Millipore-MilliQ system was used for preparing all the solutions.

2.2. Apparatus

Sonication treatments were carried out with a VCX 130W ultrasonic processor (Sonics and Materials, Inc.) of 20 kHz frequency with a titanium alloy microtip (3 mm diameter).

Scanning Electron Microscopy (SEM) images were obtained with a Field Emission Gun Scanning Electron Microscope (FE-SEM, Zeiss, Σ IGMA model) equipped with secondary and back-scattered electron detectors. The samples were obtained by casting glassy carbon disks with the MWCNTs dispersions followed by solvent evaporation at room temperature.

Uv-vis absorption spectra were obtained with a Shimadzu UV-1700 Pharma spectrophotometer using a quartz cuvette of 1 mm path length.

Electrochemical experiments were carried out with a TEQ_04 potentiostat. Glassy carbon (GCE, CH Instruments, 3mm diameter) and modified-GCE were used as working electrodes. A platinum wire and Ag/AgCl, 3 M NaCl (BAS, Model RE-5B) were used as auxiliary and reference electrodes, respectively. All potentials are referred to this reference electrode. A magnetic stirrer under controlled speed provided the convective transport during the amperometric measurements.

2.3. Preparation of MWCNTs-ConA dispersion

The MWCNTs-ConA dispersion was prepared by mixing 1.5 mg of MWCNTs with 1.0 mL of 2.0 mg mL⁻¹ ConA solution (prepared in water) followed by sonication with a sonicator probe for 5.0 min. The amplitude was 50% and the sample was kept in an ice-bath during this treatment (Figure 1A). For comparison, a dispersion of MWCNTs in water (MWCNTs-water) was prepared using the same conditions.

2.4. Preparation of glassy carbon electrodes modified with MWCNTs-ConA dispersion (GCE/MWCNTs-ConA)

GCE surfaces were polished with alumina slurries (1.0, 0.3 and 0.05 μm) for 1 min each, rinsed thoroughly with deionized water, sonicated for 30 s in water, and finally dried under a N₂ stream. GCE/MWCNTs-ConA was prepared by casting 10 μL of MWCNTs-ConA onto the glassy carbon surface, followed by the evaporation of the solvent at room temperature (Figure 1B). For comparison,

the GCE was also modified with MWCNTs dispersed in water, followed by the addition of 10 μL of 2.0 mg mL^{-1} ConA solution (prepared in water), once the solvent was evaporated (GCE/MWCNTs/ConA). The resulting bioelectrodes were exhaustively rinsed with deionized water before using.

2.5. Preparation of mono- and bienzymatic glucose biosensors

Monoenzymatic glucose biosensor (GCE/MWCNTs-ConA/GOx): The immobilization of GOx was carried out by dropping 20 μL of a 5.0 mg mL^{-1} GOx solution (prepared in a 0.050 M phosphate buffer solution pH 7.40) onto GCE/MWCNTs-ConA for 5.0 min under conditions that avoiding the solvent evaporation (Figure 1B).

Bienzymatic glucose biosensor (GCE/MWCNTs-ConA/HRP-GOx): This biosensor was prepared by dropping 20 μL of a solution containing 5.0 mg mL^{-1} GOx and 2.5 mg mL^{-1} HRP (in the same buffer) onto GCE/MWCNTs-ConA for 5.0 min under conditions that avoiding the solvent evaporation (Figure 1B).

Both biosensors were exhaustively rinsed with 0.050 M phosphate buffer solution pH 7.40 before using.

2.6. Procedure

Amperometric experiments were performed in a stirred 0.050 M phosphate buffer solution pH 7.40 by applying 0.700 V as working potential in the case of GCE/MWCNTs-ConA/GOx biosensor, and -0.050 V in a 1.0×10^{-4} M hydroquinone solution (prepared in a 0.050 M phosphate buffer solution pH 7.40)

in the case of GCE/MWCNTs-ConA/HRP-GOx. All experiments were conducted at room temperature.

2.7. Determination of glucose in real samples

A stock solution of nasal spray was prepared by dissolving the content of five doses of the spray in 5.0 mL of 0.050 M phosphate buffer solution pH 7.40. A 30 μ L-aliquot of this solution was directly transferred to the electrochemical cell containing 5.0 mL of a 0.050 M phosphate buffer solution pH 7.40, and the determination of glucose was performed by amperometry at 0.700 V using GCE/MWCNTs-ConA/GOx biosensor. Lyophilized serum was reconstituted with 5.0 mL of ultrapure water by mixing up to total dissolution according to the instructions of supplier. A 10 μ L-aliquot of this solution was directly transferred to the electrochemical cell containing 5.0 mL of 1.0×10^{-4} M hydroquinone solution (prepared in a 0.050 M phosphate buffer solution pH 7.40), and the determination of glucose was performed by amperometry at -0.050 V using GCE/MWCNTs-ConA/HRP-GOx biosensor. The quantification of glucose was accomplished by using the standard additions method in both cases.

3. RESULTS AND DISCUSSION

3.1. Characterization of MWCNTs-ConA dispersion

Figure 2A shows pictures of MWCNTs-dispersions prepared in water (a) and ConA solution (b). As can be seen, the MWCNTs-water dispersion presents a large number of aggregates due to the strong van der Waals and π - π

interactions between the nanotubes walls. On the contrary, a large decrease of these aggregates is observed in the presence of the lectin as dispersing agent since the non-covalent functionalization of MWCNTs with ConA minimizes these interactions improving their compatibility in aqueous media.

Figure 2B and C show SEM images obtained for glassy carbon disks modified with MWCNTs-water (B) and MWCNTs-ConA (C) dispersions. In the case of the water-dispersed MWCNTs, there is a large number of aggregates of MWCNTs as a consequence of their poor dispersion (see Fig 2A,a), at variance with the glassy carbon surface covered by MWCNTs dispersed in ConA where the MWCNTs are efficiently entrapped within the lectin net, decreasing, in this way, the number of aggregates.

Figure SI-1 displays UV-vis spectra for Con A solution before (a), and after sonication in the presence of MWCNTs followed by the separation of MWCNTs-ConA by centrifugation at 12000 rpm for 15 min (b). The spectrum of native ConA shows an absorption band centered at 277 nm due to the absorption of the aromatic amino acids residues [26]. After sonication of MWCNTs with ConA and separation of MWCNTs-ConA by centrifugation, it was observed a slight red-shift in the wavelength of maximum absorption (279 nm), probably due to some degree of denaturation of the lectin by the effect of ultrasound energy and an obvious decrease in the maximum absorption. These results indicate in an indirect way, that ConA was bound to MWCNTs (in addition to the confirmation through the interaction with glycoenzymes discussed in the following sections). The interaction between MWCNTs and ConA could be established between the π -system of nanotubes and the cavities of the protein rich in hydrophobic aminoacids [10,27]. The amount of Con A immobilized at MWCNTs, estimated

from the difference between the maximum absorbance of the polypeptide chains-band for the ConA solution before and after the interaction with MWCNTs and separation of MWCNTs-Con A, was 0.72 mg per mg of MWCNTs.

To evaluate if ConA retains its unique properties for the specific recognition of glycoproteins even after the sonication step during the preparation of the dispersion, we studied the interaction of GCW/MWCNTs-ConA with GOx as a model glycoenzyme. Figure 3A shows a cyclic voltammogram obtained in a 0.050 M phosphate buffer solution pH 7.40 at 0.050 V s⁻¹ for GCE/MWCNTs-ConA/GOx. A well-defined quasi-reversible redox peaks-system, due to the reduction/oxidation of the prosthetic group of the enzyme (FAD), is observed at -0.437 V (anodic peak) and -0.507 V (cathodic peak), with a peak potential separation of 70 mV and a formal potential of -0.472 V. These values are in agreement with those reported in the literature [28–30]. No redox peaks system was observed when GOx was allowed to interact with GCE/MWCNTs (without ConA) (not shown). These results clearly indicate that the ConA that supports the carbon nanostructures allows the recognition of GOx even after the sonication treatment used to prepare the dispersion, and this intimate contact between lectin and enzyme, makes possible the direct electron transfer between the FAD center of the enzyme and the electrode surface. The linear relationship between the cathodic and anodic peaks currents and the scan rate in the range between 0.010 and 0.100 V s⁻¹ confirms that the reduction/oxidation of FAD/FADH₂ is a surface-controlled quasi-reversible process (inset in Figure 3A). The average surface concentration (Γ) of electroactive GOx present in GCE/MWCNTs-ConA/GOx was estimated according to the following equation:

$$i_p = n^2 F^2 v \Gamma A / 4RT$$

where v is the scan rate, n is the number of the electrons involved in the redox process, F is the Faraday constant, A is the effective area of the electrode, R is the gas constant, and T is the temperature. This average coverage was $2.33 \times 10^{-11} \text{ mol cm}^{-2}$. As control, the average coverage obtained at GCE/MWCNTs/ConA/GOx was $1.07 \times 10^{-11} \text{ mol cm}^{-2}$, that is 2.2 times lower than the one obtained at GCE/MWCNTs-ConA/GOx, thus, confirming the increased glycoprotein loading when MWCNTs are dispersed in ConA.

Figure 3B displays cyclic voltammograms for GCE/MWCNTs-ConA/GOx in N_2 -saturated 0.050 M phosphate buffer solution pH 7.40 containing $5.0 \times 10^{-4} \text{ M}$ ferrocene methanol without (black curve, a) and with (red curve, b) $5.0 \times 10^{-2} \text{ M}$ glucose. In the absence of glucose, a quasi-reversible peaks-system is observed due to the redox behavior of ferrocene methanol, while in the presence of glucose the anodic peak current largely increases and the cathodic one decreases, as expected for the biocatalytic activity of GOx. The surface coverage of bioactive GOx (Γ_{GOx}^*) present at the GCE/MWCNTs-ConA/GOx was calculated according to the Bourdillon method using the following equation [31]:

$$i_{\text{cat}} = \frac{nFAk_3\Gamma_{\text{GOx}}^*[\text{FcMO}^{\cdot+}]}{1 + k_3[\text{FcMO}^{\cdot+}]\left(\frac{1}{k_2} + \frac{1}{k_{\text{red}}[\text{Glu}]}\right)}$$

where $[\text{FcMOH}^{\cdot+}]$ and $[\text{Glu}]$ are the concentrations of the oxidized mediator and substrate, respectively; $k_{\text{red}} = k_1k_2/(k_{-1} + k_2)$, and i_{cat} , is the catalytic current determined at GCE/MWCNTs-ConA/GOx as the difference between the current obtained in the absence and presence of $5.0 \times 10^{-2} \text{ M}$ glucose. The constant values used for the calculation were $k_2 = 780 \text{ s}^{-1}$, $k_3 = (6.2 \pm 0.5) \times 10^{-6} \text{ M}^{-1} \text{ s}^{-1}$, and $k_{\text{red}} = 1.2 \times 10^4 \text{ M}^{-1} \text{ s}^{-1}$. Under our experimental conditions, Γ_{GOx} was $4.2 \times 10^{-12} \text{ mol cm}^{-2}$ (assuming a two-electron transfer reaction), which corresponds to

18% of the average coverage of electroactive GOx. These results clearly indicate that GCE/MWCNTs-ConA allows the specific recognition of the glycoenzyme retaining its biocatalytic activity and opening the doors for the development of glucose biosensors.

3.2. Optimization of MWCNTs-ConA dispersion and construction of the glucose biosensors

The optimization of the experimental conditions for the preparation of MWCNTs-ConA dispersion (amount of MWCNTs, concentration of ConA and sonication time) was performed in two ways. In the first one, we evaluated the effectiveness of the dispersion through the amperometric response of H₂O₂ at 0.700 V by using GCE/MWCNTs-ConA. In the second one, we evaluated the biorecognition properties of MWCNTs-ConA through the amperometric response of glucose at 0.700 V by using GCE/MWCNTs-ConA/GOx. The potential of 0.700 V was selected from the evaluation of the voltammetric response obtained in the presence of 2.0×10^{-2} M glucose at GCE/MWCNTs-ConA/GOx (See Figure SI-2).

Figure 4 shows the effect of the amount of MWCNTs present in the MWCNTs-ConA dispersion on the sensitivity for H₂O₂ (A) and glucose (B), obtained from amperometric experiments performed at 0.700 V using GCE modified with MWCNTs-ConA dispersions prepared by sonication of different amounts of MWCNTs (0.5, 1.0, 1.5 and 2.0 mg) in 1.0 mL of 2.0 mg mL^{-1} ConA (prepared in water) for 5.0 min. Both sensitivities increase up to 1.5 mg of MWCNTs and level off or slightly decreases thereafter, suggesting that the amount of lectin is not enough to disperse larger amounts of nanotubes. Then,

1.5 mg of MWCNT was selected for preparing further MWCNTs-ConA dispersions.

The concentration of dispersing agent is an important parameter that influences the efficiency of MWCNTs dispersions since it works as spacer between the nanotubes [32]. The effect of the concentration of ConA used to prepare the MWCNTs dispersions was evaluated in the range between 0 and 3.0 mg mL⁻¹ (Figure 4C-D). The sensitivities to H₂O₂ and glucose increase up to 2.0 mg mL⁻¹ and level off thereafter. Higher concentration of ConA produces a small decrease in the sensitivities which is attributed to the blockage of the electrode surface. According to these results, we selected 2.0 mg mL⁻¹ ConA to obtain the most efficient carbon nanotubes dispersion with the best biorecognition conditions to immobilize the glycoenzyme GOx.

The time of ultrasonic treatment during the preparation of the dispersion is another important parameter. The sonication time should be high enough to allow the separation of the nanotubes as a consequence of the intimate interaction between the lectin and nanotube walls, but not too high that completely denature the Con A. Figure 4 shows the sensitivities for H₂O₂ (E) and glucose (F) obtained using GCE modified with MWCNTs-ConA dispersions prepared using different sonication times (0, 1.0, 2.5, 5.0 and 7.5 min). A period of 5.0 min sonication was the best to obtain the highest sensitivity either in the case of hydrogen peroxide (A) or glucose (B). Longer times were not beneficial probably due to some change in the characteristics of the lectin that make the dispersion less efficient. Therefore, 5.0 min was selected as optimal to prepare the MWCNTs-ConA dispersions.

The interaction time between GOx and GCE/MWCNTs-ConA and the concentration of GOx were also optimized through the amperometric response of glucose. Figure SI-3A shows the sensitivities for glucose obtained at GCE/MWCNTs-ConA/GOx biosensors prepared through the interaction of a 5.0 mg mL⁻¹ GOx solution with GCE/MWCNTs-ConA for different times (1.0, 2.0, 5.0 and 30.0 min). As can be seen, just one minute is enough to reach the highest sensitivity, demonstrating the excellent biorecognition properties of the immobilized ConA. An incubation time of 5.0 min was selected as a compromise between the highest sensitivity and the best reproducibility. It is also interesting to remark that the sensitivity of the biosensor increased progressively with the concentration of the enzyme, reaching the highest value for a 5.0 mg mL⁻¹ GOx solution (Figure SI-3B).

3.3. Analytical performance of the glucose biosensors (GCE/MWCNTs-ConA/GOx and GCE/MWCNTs-ConA/HRP-GOx)

Figure 5 displays the amperometric response obtained under the optimal conditions at GCE/MWCNTs-ConA/GOx for successive additions of glucose in a stirred 0.050 M phosphate buffer solution pH 7.40 at 0.700 V (A), and the resulting calibration plot (B). A clearly defined and fast (5 seconds) response is obtained after the addition of micromolar levels of glucose, evidencing an efficient transduction of the biorecognition event by the bioanalytical platform. The calibration plot shows a linear range from 5.0 x 10⁻⁶ M to 1.2 x 10⁻³ M ($r^2=0.997$), with a sensitivity of (2.22 ± 0.03) μA mM⁻¹, and a limit of detection of 1.6 μM (taken as 3.3 σ/S, where σ is the standard deviation of the blank signal and S the sensitivity).

The reproducibility obtained with five GCE/MWCNTs-ConA/GOx biosensors prepared with the same dispersion was 6.8%, while the reproducibility obtained with eleven GCE/MWCNTs-ConA/GOx biosensors prepared with eleven MWCNTs-ConA dispersions obtained in different days was 9.2%. The repeatability of GCE/MWCNTs-ConA/GOx, obtained from five consecutive glucose determinations, was 3.0%. The reproducibility and repeatability were calculated from the sensitivity to glucose obtained from amperometric experiments. The stability of the MWCNTs-ConA dispersion was evaluated from the sensitivity to glucose performed with GCE/MWCNTs-ConA/GOx biosensors prepared each testing day with a MWCNTs-ConA dispersion stored at 4 °C. Negligible changes were obtained in the sensitivity to glucose during 33 days, with a loss of sensitivity of 20% after 44 days and 22% after the 65th day, demonstrating the high stability of MWCNTs-ConA dispersion.

The selectivity of GCE/MWCNTs-ConA/GOx was evaluated in the presence of 2.5×10^{-4} M fructose, galactose, maltose and lactose, and no interference was observed in any case (not shown). The glucose content in a nasal spray, which contains glucose as excipient, was evaluated as real application for GCE/MWCNTs-ConA/GOx biosensor. The concentration of glucose, obtained from 6 determinations, was (2.78 ± 0.09) mg per dose, showing an excellent agreement with the value reported in the pharmaceutical product (2.75 mg of glucose per dose), demonstrating the usefulness of GCE/MWCNTs-ConA/GOx for the quantification of glucose in this medicine sample.

However, even when this biosensor present competitive analytical characteristics, it has the inconvenience of the interference of uric acid (UA) and ascorbic acid (AA) due to the high working potential. In fact, in the determination

of 2.5×10^{-4} M glucose, there is an interference of 23 % for 5.0×10^{-6} M AA and 76 % for 2.5×10^{-5} M UA. The incorporation of a layer of 1.0% Nafion solution (prepared in 0.050 M phosphate buffer pH 7.40) at GCE/MWCNTs-ConA/GOx decreased the interferences to 4.5% and 22% for AA and UA, respectively.

To overcome this problem, we investigated the co-immobilization of two glycoenzymes, HRP and GOx at the surface of GCE/MWCNTs-ConA to build a glucose bienzymatic platform (GCE/MWCNTs-ConA/HRP-GOx). The analytical signal for GCE/MWCNTs-ConA/HRP-GOx was obtained from amperometric experiments at -0.050 V by using 1.0×10^{-4} M hydroquinone as redox mediator. The working potential was selected from the voltammetric response obtained at GCE/MWCNTs-ConA/HRP-GOx in the absence and presence of 2.0×10^{-2} M glucose in a solution containing 1.0×10^{-4} M hydroquinone (See Figure SI-4).

GOx/HRP ratio used to prepare GCE/MWCNTs-ConA/HRP-GOx is a critical aspect for the analytical performance of the biosensor. Figure 6A shows the variation of the sensitivity to glucose obtained for bienzymatic biosensors prepared with a constant concentration of HRP (2.5 mg mL^{-1}) and different concentrations of GOx, while Figure 6B displays the effect of GOx/HRP ratio for a constant GOx concentration (5.0 mg mL^{-1}) and different concentrations of HRP. The maximum sensitivity was obtained when using 5.0 mg mL^{-1} GOx and 2.5 mg mL^{-1} HRP, therefore, these enzyme concentrations were selected for the bienzymatic biosensor preparation.

Figure 7A shows the amperometric response obtained at optimized GCE/MWCNTs-ConA/HRP-GOx at - 0.050 V for successive additions of glucose in a stirred 1.0×10^{-4} M hydroquinone solution (prepared in a 0.050 M phosphate buffer solution pH 7.40), while Figure 7B displays the corresponding calibration

curve. A fast and even better defined amperometric response is obtained after the successive additions of glucose (compared to the monoenzymatic biosensor). The bienzymatic biosensor presents a linear range between 2.0×10^{-6} M and 4.1×10^{-4} M ($r^2=0.9998$), covering two orders of magnitude, with a sensitivity of $(11.5 \pm 0.4) \mu\text{A mM}^{-1}$, which is 5.2 times higher than that obtained at GCE/MWCNTs-ConA/GOx biosensor ($(2.22 \pm 0.03) \mu\text{A mM}^{-1}$). Moreover, the limit of detection (taken as indicated before) was estimated to be $0.31 \mu\text{M}$, that is almost one order of magnitude lower than that obtained with the monoenzymatic biosensor ($1.6 \mu\text{M}$). The limit of detection obtained with our bienzymatic biosensor was lower or comparable to the ones of most of the enzymatic glucose biosensors based on the H_2O_2 reduction reported in the last years (Table 1). Therefore, GCE/MWCNTs-ConA/HRP-GOx allow to work at lower potentials, with increased sensitivity and selectivity,

The sensitivities obtained with five different GCE/MWCNTs-ConA/HRP-GOx biosensors showed a RSD value of 5.4%, indicating an excellent reproducibility in the whole preparation process of the bioanalytical platform. In addition to the significant increment in sensitivity, the bienzymatic biosensor presents the great advantage of using a low working potential for the amperometric detection of glucose, allowing in this way the elimination of the interference produced by ascorbic and uric acids, thus improving the selectivity of the biosensor (Figure SI-5).

To demonstrate the usefulness of the proposed bienzymatic biosensor in a complex matrix, we quantify glucose in blood human serum samples. The average concentration of glucose obtained from 4 determinations was $(0.84 \pm 0.04) \text{ g/L}$, that is in excellent agreement with the value reported by Wiener

laboratory (0.87 g/L). These results demonstrate once more the advantages of the bienzymatic biosensor that allows to work at considerably lower potentials, largely decreasing the interference of easily oxidizable compounds, and allowing, in this way, the use of biosensor for the quantification of glucose in complex samples like human blood serum without any pretreatment.

4. CONCLUSIONS

We demonstrate here that, at variance with previous reports, MWCNTs can be non-covalently functionalized with ConA in a direct way just by sonicating them in the presence of ConA. The resulting MWCNTs-ConA dispersion was successfully used as building block to develop biosensors through the supramolecular site-specific recognition of glycobiomolecules. In this case, as proof-of-concept, we developed glucose biosensors based on the immobilization of two glycoproteins, GOx and HRP, to prepare either mono- and bienzymatic biosensors. The advantages of the cascade reactions at GCE/MWCNTs-ConA/HRP-GOx between glucose/GOx and hydrogen peroxide/HRP mediated by hydroquinone was clearly demonstrated through the important increase in the sensitivity to glucose, the significant improvement in the selectivity and the successful application in complex matrices like human blood serum.

In summary, MWCNTs-ConA represents a very attractive platform for the development of different biosensing strategies either by specific-anchoring of a selected glycobiomolecule able to be used as biorecognition element, by direct quantification of relevant glycoproteins or bacteria, or by using the MWCNTs-ConA bioconjugate for designing innovative amplification schemes.

ACKNOWLEDGEMENTS

The authors thank CONICET (PIP 2015), SECyT-UNC (2018-2021), and FONCyT (PICT 2016-1261 and PICT 2016-1306) for the financial support. P. G. and E.O. acknowledge the fellowships to CONICET and CONACyT, respectively.

ACCEPTED MANUSCRIPT

5. REFERENCES

- [1] C. Zhu, G. Yang, H. Li, D. Du, Y. Lin, Electrochemical sensors and biosensors based on nanomaterials and nanostructures, *Anal. Chem.* 87 (2015) 230–249. doi:10.1021/ac5039863.
- [2] G. Maduraiveeran, M. Sasidharan, V. Ganesan, Electrochemical sensor and biosensor platforms based on advanced nanomaterials for biological and biomedical applications, *Biosens. Bioelectron.* 103 (2018) 113–129. doi:10.1016/j.bios.2017.12.031.
- [3] I. V. Zaporotskova, N.P. Boroznina, Y.N. Parkhomenko, L. V. Kozhitov, Carbon nanotubes: Sensor properties. A review, *Mod. Electron. Mater.* 2 (2016) 95–105. doi:10.1016/j.moem.2017.02.002.
- [4] G.A. Rivas, M.C. Rodríguez, M.D. Rubianes, F.A. Gutierrez, M. Eguílaz, P.R. Dalmasso, E.N. Primo, C. Tettamanti, M.L. Ramírez, A. Montemerlo, P. Gallay, C. Parrado, Carbon nanotubes-based electrochemical (bio)sensors for biomarkers, *Appl. Mater. Today.* 9 (2017) 566–588. doi:10.1016/j.apmt.2017.10.005.
- [5] S. Mallakpour, S. Soltanian, Surface functionalization of carbon nanotubes: Fabrication and applications, *RSC Adv.* 6 (2016) 109916–109935. doi:10.1039/c6ra24522f.
- [6] E.N. Primo, F.A. Gutiérrez, G.L. Luque, P.R. Dalmasso, A. Gasnier, Y. Jalit, M. Moreno, M. V. Bracamonte, M.E. Rubio, M.L. Pedano, M.C. Rodríguez, N.F. Ferreyra, M.D. Rubianes, S. Bollo, G.A. Rivas, Comparative study of the electrochemical behavior and analytical applications of (bio)sensing platforms based on the use of multi-walled carbon nanotubes dispersed in

- different polymers, *Anal. Chim. Acta.* 805 (2013) 19–35. doi:10.1016/j.aca.2013.10.039.
- [7] P. Bilalis, D. Katsigiannopoulos, A. Avgeropoulos, G. Sakellariou, Non-covalent functionalization of carbon nanotubes with polymers, *RSC Adv.* 4 (2014) 2911–2934. doi:10.1039/c3ra44906h.
- [8] Y. Zhou, Y. Fang, R.P. Ramasamy, Non-covalent functionalization of carbon nanotubes for electrochemical biosensor development, *Sensors (Switzerland)*. 19 (2019) 902–930. doi:10.3390/s19020392.
- [9] M. Eguílaz, A. Gutiérrez, G. Rivas, Non-covalent functionalization of multi-walled carbon nanotubes with cytochrome c: Enhanced direct electron transfer and analytical applications, *Sensors Actuators B Chem. B Chem.* 225 (2016) 74–80. doi:10.1016/j.snb.2015.11.011.
- [10] K.E. Sapsford, W.R. Algar, L. Berti, K.B. Gemmill, B.J. Casey, E. Oh, M.H. Stewart, I.L. Medintz, Functionalizing Nanoparticles with Biological Molecules: Developing Chemistries that Facilitate Nanotechnology, *Chem. Rev.* 113 (2013) 1904–2074. doi:10.1021/cr300143v.
- [11] Y. Liu, J. Yu, Oriented immobilization of proteins on solid supports for use in biosensors and biochips: a review, *Microchim. Acta.* 183 (2016) 1–19. doi:10.1007/s00604-015-1623-4.
- [12] J.I. Reyes-De-Corcuera, H.E. Olstad, R. García-Torres, Stability and Stabilization of Enzyme Biosensors: The Key to Successful Application and Commercialization, *Annu. Rev. Food Sci. Technol.* 9 (2018) 293–322. doi:10.1146/annurev-food-030216-025713.
- [13] B. Wang, J.I. Anzai, Recent progress in lectin-based biosensors, *Materials (Basel)*. 8 (2015) 8590–8607. doi:10.3390/ma8125478.

- [14] L. Zhao, C. Li, H. Qi, Q. Gao, C. Zhang, Electrochemical lectin-based biosensor array for detection and discrimination of carcinoembryonic antigen using dual amplification of gold nanoparticles and horseradish peroxidase, *Sensors Actuators, B Chem.* 235 (2016) 575–582. doi:10.1016/j.snb.2016.05.136.
- [15] U. Akiba, J.I. Anzai, Recent Progress in Electrochemical Biosensors for Glycoproteins, *Sensors (Basel)*. 16 (2016) 1–18. doi:10.3390/s16122045.
- [16] J. Filip, S. Zavahir, L. Klukova, J. Tkac, P. Kasak, Immobilization of concanavalin A lectin on a reduced graphene oxide-thionine surface by glutaraldehyde crosslinking for the construction of an impedimetric biosensor, *J. Electroanal. Chem.* 794 (2017) 156–163. doi:10.1016/j.jelechem.2017.04.019.
- [17] X. Ou, X. Tan, X. Liu, Q. Lu, S. Chen, S. Wei, A signal-on electrochemiluminescence biosensor for detecting Con A using phenoxy dextran-graphite-like carbon nitride as signal probe, *Biosens. Bioelectron.* 70 (2015) 89–97. doi:10.1016/j.bios.2015.03.021.
- [18] S.A. Hong, J. Kwon, D. Kim, S. Yang, A rapid, sensitive and selective electrochemical biosensor with concanavalin A for the preemptive detection of norovirus, *Biosens. Bioelectron.* 64 (2015) 338–344. doi:10.1016/j.bios.2014.09.025.
- [19] A.D. Chowdhury, A.B. Ganganboina, E.Y. Park, R. an Doong, Impedimetric biosensor for detection of cancer cells employing carbohydrate targeting ability of Concanavalin A, *Biosens. Bioelectron.* 122 (2018) 95–103. doi:10.1016/j.bios.2018.08.039.
- [20] D. Pallarola, N. Queralto, F. Battaglini, O. Azzaroni, Supramolecular

- assembly of glucose oxidase on concanavalin A-modified gold electrodes, *Phys. Chem. Chem. Phys.* 12 (2010) 8071–8083. doi:10.1039/c000797h.
- [21] L. Zhou, Y. Jiang, J. Gao, X. Zhao, L. Ma, Q. Zhou, Oriented immobilization of glucose oxidase on graphene oxide, *Biochem. Eng. J.* 69 (2012) 28–31. doi:10.1016/j.bej.2012.07.025.
- [22] Y. Xue, L. Bao, X. Xiao, L. Ding, J. Lei, H. Ju, Noncovalent functionalization of carbon nanotubes with lectin for label-free dynamic monitoring of cell-surface glycan expression, *Anal. Biochem.* 410 (2011) 92–97. doi:10.1016/j.ab.2010.11.019.
- [23] W. Li, R. Yuan, Y. Chai, H. Zhong, Y. Wang, Study of the biosensor based on platinum nanoparticles supported on carbon nanotubes and sugar-lectin biospecific interactions for the determination of glucose, *Electrochim. Acta.* 56 (2011) 4203–4208. doi:10.1016/j.electacta.2011.01.095.
- [24] Y. Li, X. Huang, Y. Qu, A strategy for efficient immobilization of laccase and horseradish peroxidase on single-walled carbon nanotubes, *J. Chem. Technol. Biotechnol.* 88 (2013) 2227–2232. doi:10.1002/jctb.4091.
- [25] V. Papper, K. Elouarzaki, K. Gorgy, A. Sukharaharja, S. Cosnier, R.S. Marks, Biofunctionalization of multiwalled carbon nanotubes by electropolymerized poly(pyrrole-concanavalin A) films, *Chem. - A Eur. J.* 20 (2014) 13561–13564. doi:10.1002/chem.201402971.
- [26] V.D. Suryawanshi, L.S. Walekar, A.H. Gore, P. V. Anbhule, G.B. Kolekar, Spectroscopic analysis on the binding interaction of biologically active pyrimidine derivative with bovine serum albumin, *J. Pharm. Anal.* 6 (2016) 56–63. doi:10.1016/j.jpha.2015.07.001.
- [27] M. Calvaresi, F. Zerbetto, Baiting Proteins with C₆₀, *ACS Nano.* 4 (2010)

- 2283–2299. doi:10.1021/nn901809b.
- [28] F. Gutierrez, M.D. Rubianes, G.A. Rivas, Dispersion of multi-wall carbon nanotubes in glucose oxidase: Characterization and analytical applications for glucose biosensing, *Sensors Actuators, B Chem.* 161 (2012) 191–197. doi:10.1016/j.snb.2011.10.010.
- [29] Y. Yu, Z. Chen, S. He, B. Zhang, X. Li, M. Yao, Direct electron transfer of glucose oxidase and biosensing for glucose based on PDDA-capped gold nanoparticle modified graphene/multi-walled carbon nanotubes electrode, *Biosens. Bioelectron.* 52 (2014) 147–152. doi:10.1016/j.bios.2013.08.043.
- [30] Z. Kang, K. Jiao, C. Yu, J. Dong, R. Peng, Z. Hu, S. Jiao, Direct electrochemistry and bioelectrocatalysis of glucose oxidase in CS/CNC film and its application in glucose biosensing and biofuel cells, *RSC Adv.* 7 (2017) 4572–4579. doi:10.1039/C6RA26636C.
- [31] C. Bourdillon, C. Demaille, J. Moiroux, J.-M. Saveant, New Insights into the Enzymatic Catalysis of the Oxidation of Glucose by Native and Recombinant Glucose Oxidase Mediated by Electrochemically Generated One-Electron Redox Cosubstrates, *J. Am. Chem. Soc.* 115 (1993) 2–10.
- [32] M. Eguílaz, N.F. Ferreyra, G.A. Rivas, Dispersions of Hollow and Bamboo-Like Multiwalled Carbon Nanotubes in Polyethyleneimine: Critical Analysis of the Preparation Conditions and Applications for Electrochemical Sensing, *Electroanalysis.* 26 (2014) 2434–2444. doi:10.1002/elan.201400298.
- [33] M. Eguílaz, C.J. Venegas, A. Gutiérrez, G.A. Rivas, S. Bollo, Carbon nanotubes non-covalently functionalized with cytochrome c: A new bioanalytical platform for building bienzymatic biosensors, *Microchem. J.*

- 128 (2016) 161–165. doi:10.1016/j.microc.2016.04.018.
- [34] Y.N. Ning, B.L. Xiao, N.N. Niu, A.A. Moosavi-Movahedi, J. Hong, Glucose oxidase immobilized on a functional polymer modified glassy carbon electrode and its molecule recognition of glucose, *Polymers (Basel)*. 11 (2019). doi:10.3390/polym11010115.
- [35] F. Wang, W. Gong, L. Wang, Z. Chen, Enhanced amperometric response of a glucose oxidase and horseradish peroxidase based bienzyme glucose biosensor modified with a film of polymerized toluidine blue containing reduced graphene oxide, *Microchim. Acta*. 182 (2015) 1949–1956. doi:10.1007/s00604-015-1535-3.
- [36] D. Manoj, K. Theyagarajan, D. Saravanakumar, S. Senthilkumar, K. Thenmozhi, Aldehyde functionalized ionic liquid on electrochemically reduced graphene oxide as a versatile platform for covalent immobilization of biomolecules and biosensing, *Biosens. Bioelectron.* 103 (2018) 104–112. doi:10.1016/j.bios.2017.12.030.
- [37] M. David, M.M. Barsan, C.M.A. Brett, M. Florescu, Improved glucose label-free biosensor with layer-by-layer architecture and conducting polymer poly(3,4-ethylenedioxythiophene), *Sensors Actuators, B Chem.* 255 (2018) 3227–3234. doi:10.1016/j.snb.2017.09.149.
- [38] H. Tang, D. Cai, T. Ren, P. Xiong, Y. Liu, H. Gu, G. Shi, Fabrication of a low background signal glucose biosensor with 3D network materials as the electrocatalyst, *Anal. Biochem.* 567 (2019) 63–71. doi:10.1016/j.ab.2018.12.012.
- [39] Q. Guo, L. Liu, T. Wu, Q. Wang, H. Wang, J. Liang, S. Chen, Flexible and conductive titanium carbide–carbon nanofibers for high-performance

- glucose biosensing, *Electrochim. Acta.* 281 (2018) 517–524.
doi:10.1016/j.electacta.2018.05.181.
- [40] H. Xia, Y. Kitazumi, O. Shirai, K. Kano, Direct Electron Transfer-type Bioelectrocatalysis of Peroxidase at Mesoporous Carbon Electrodes and Its Application for Glucose Determination Based on Bienzyme System, *Anal. Sci.* 33 (2017) 839–844. doi:10.2116/analsci.33.839.
- [41] Q. Guo, L. Liu, M. Zhang, H. Hou, Y. Song, H. Wang, B. Zhong, L. Wang, Hierarchically mesostructured porous TiO₂ hollow nanofibers for high performance glucose biosensing, *Biosens. Bioelectron.* 92 (2017) 654–660. doi:10.1016/j.bios.2016.10.036.
- [42] L. Wang, J. Li, M. Feng, L. Min, J. Yang, S. Yu, Y. Zhang, X. Hu, Z. Yang, Perovskite-type calcium titanate nanoparticles as novel matrix for designing sensitive electrochemical biosensing, *Biosens. Bioelectron.* 96 (2017) 220–226. doi:10.1016/j.bios.2017.05.004.
- [43] W. Mao, B. Cai, Z. Ye, J. Huang, A nanostructured p-NiO/n-Bi₄Ti₃O₁₂ heterojunction for direct GOx electrochemistry and high-sensitivity glucose sensing, *Sensors Actuators, B Chem.* 261 (2018) 385–391. doi:10.1016/j.snb.2018.01.138.

LEGENDS OF THE FIGURES

Figure 1: Schematic representation of the steps involved in the preparation of the glucose biosensors.

Figure 2: (A) Pictures of MWCNTs dispersions prepared in water (a) and ConA solution (b), obtained by ultrasonication for 5.0 min. SEM micrograph of glassy carbon disk modified with dispersions of MWCNTs-water (B) and MWCNTs-ConA (C). Magnification: 3810X. The insets corresponds to SEM micrographs at higher magnification (22870X).

Figure 3:

(A) Cyclic voltammogram obtained at GCE/MWCNTs-ConA in a solution of N₂-saturated 0.050 M phosphate buffer solution pH 7.40. Scan rate: 0.100 Vs⁻¹. Inset: Dependence of peak currents on the scan rates. (B) Cyclic voltammograms for 5.0 x 10⁻⁴ M ferrocene methanol at GCE/MWCNTs-ConA/GOx in a N₂-saturated 0.050 M phosphate buffer solution pH 7.40 without (black curve) and with 0.050 M glucose (red curve). Scan rate: 0.005 Vs⁻¹.

Figure 4: Variation of the sensitivity obtained from amperometric experiments performed at GCE/MWCNTs-ConA for H₂O₂ (A, C, E), and at GCE/MWCNTs-ConA/GOx for glucose (B, D, F) as a function of the amount of MWCNTs (A, B), ConA concentration (C, D) and sonication time (E, F) used to prepare MWCNTs-ConA. Working potential: 0.700 V.

Figure 5: (A) Amperometric recording for successive additions of glucose at GCE/MWCNTs-ConA/GOx: (a) 5.0×10^{-6} M, (b) 1.0×10^{-5} M, (c) 5.0×10^{-5} M, and (e) 1.0×10^{-4} M. (B) Calibration plot obtained from the amperometric recording shown in Figure 5A. Supporting electrolyte: 0.050 M phosphate buffer solution pH 7.40. Working potential: 0.700 V.

Figure 6: Variation of the glucose sensitivity as a function of the concentration of (A) HRP and (B) GOx used to prepare GCE/MWCNTs-ConA/HRP-GOx. Supporting electrolyte: 0.050 M phosphate buffer solution pH 7.40, containing 1.0×10^{-4} M hydroquinone. Working potential: -0.050 V.

Figure 7: (A) Amperometric recording for successive additions of glucose at GCE/MWCNTs-ConA/HRP-GOx: (a) 2.0×10^{-6} M, (b) 5.0×10^{-6} M, (c) 1.0×10^{-5} M, (d) 5.0×10^{-5} M, and (e) 1.0×10^{-4} M. (B) Calibration plot obtained from the amperometric recording shown in Figure 7A. Supporting electrolyte: 0.050 M phosphate buffer solution pH 7.40, containing 1.0×10^{-4} M hydroquinone. Working potential: -0.050 V.

FIGURE 1- Rivas ET AL.

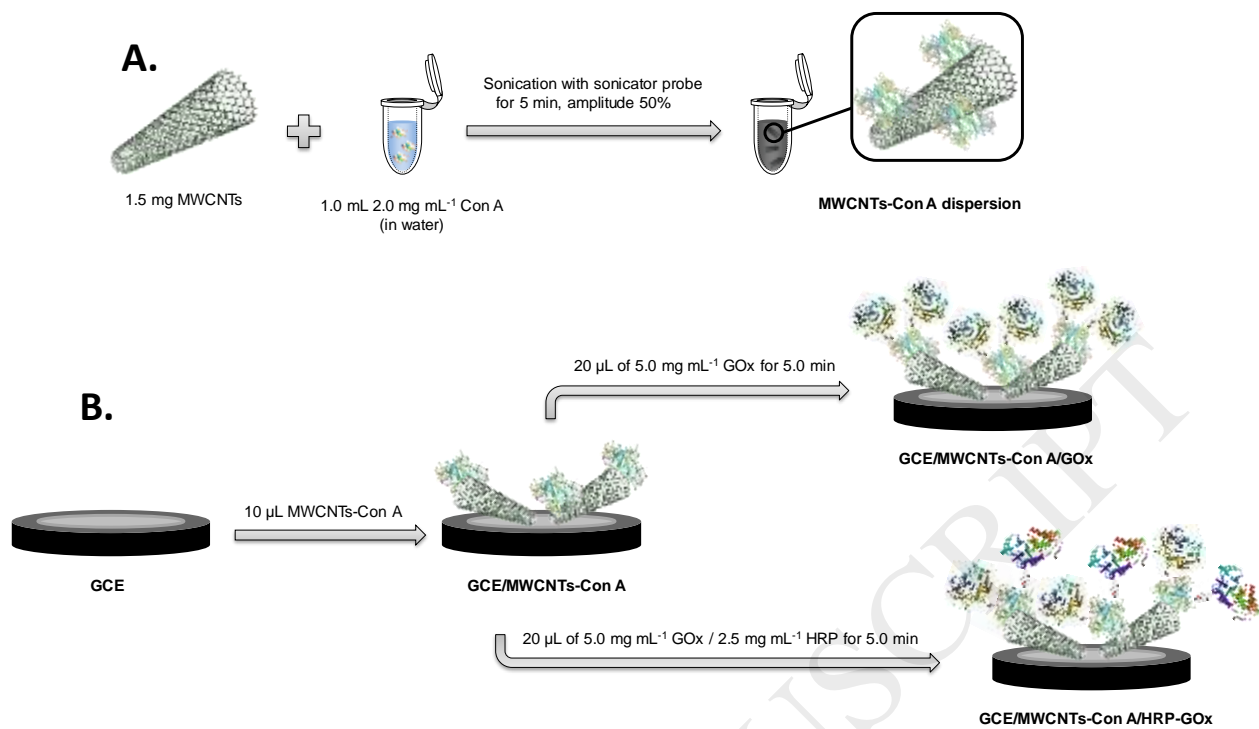


FIGURE 2- Rivas ET AL.

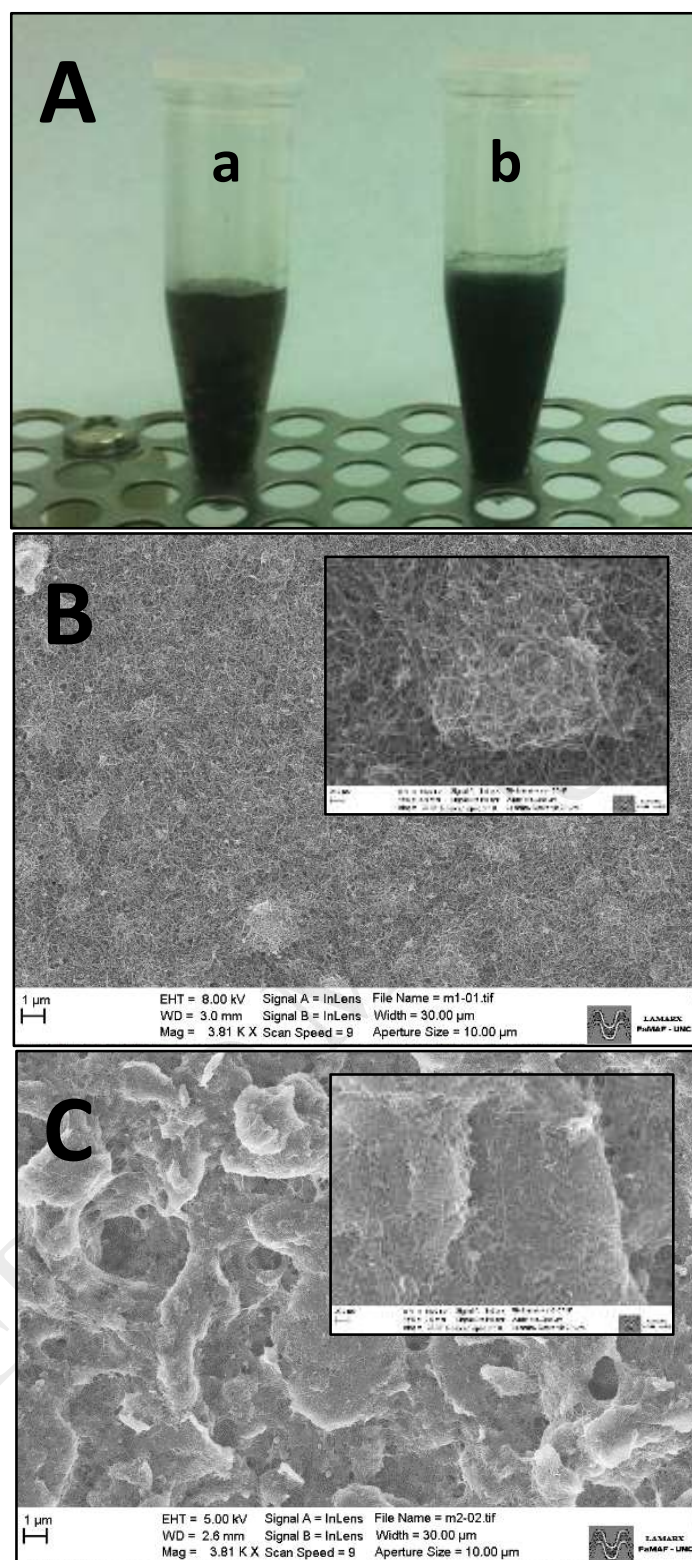


FIGURE 3- Rivas ET AL.

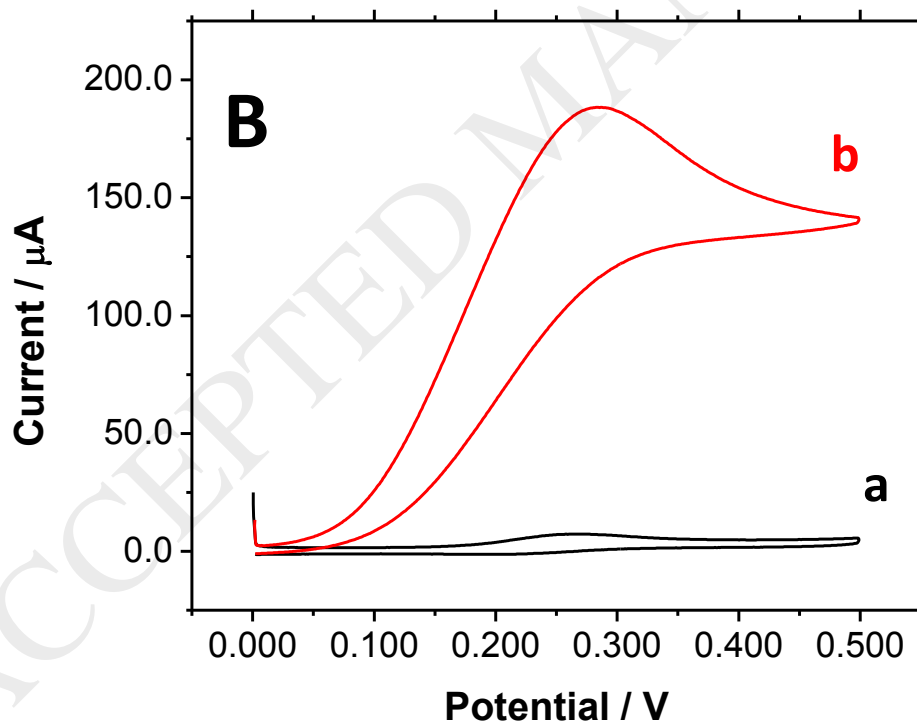
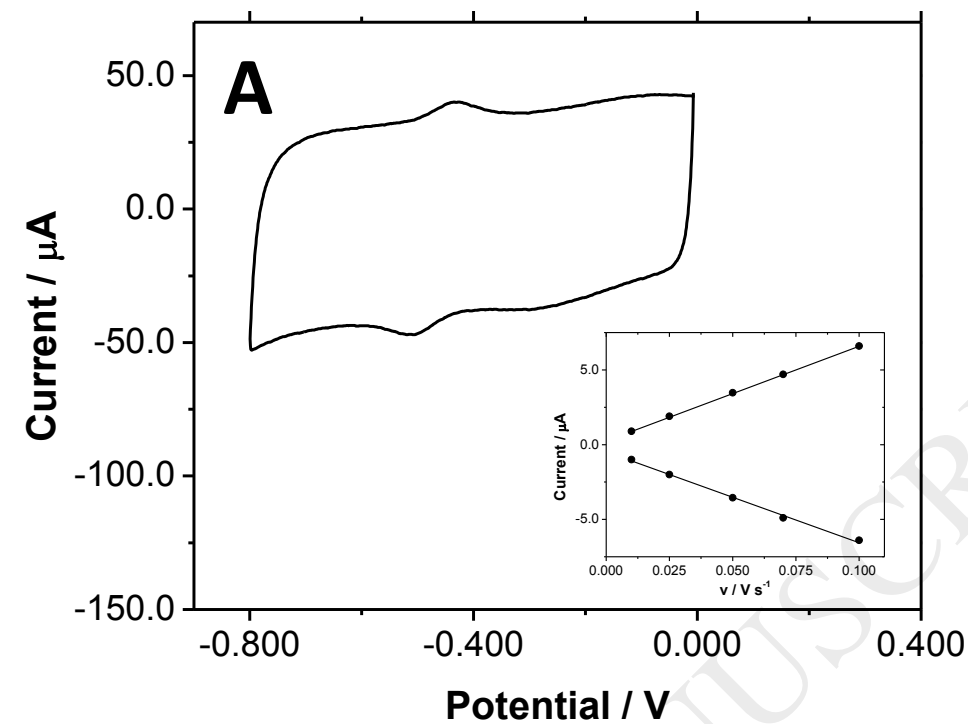


FIGURE 4- Rivas ET AL.

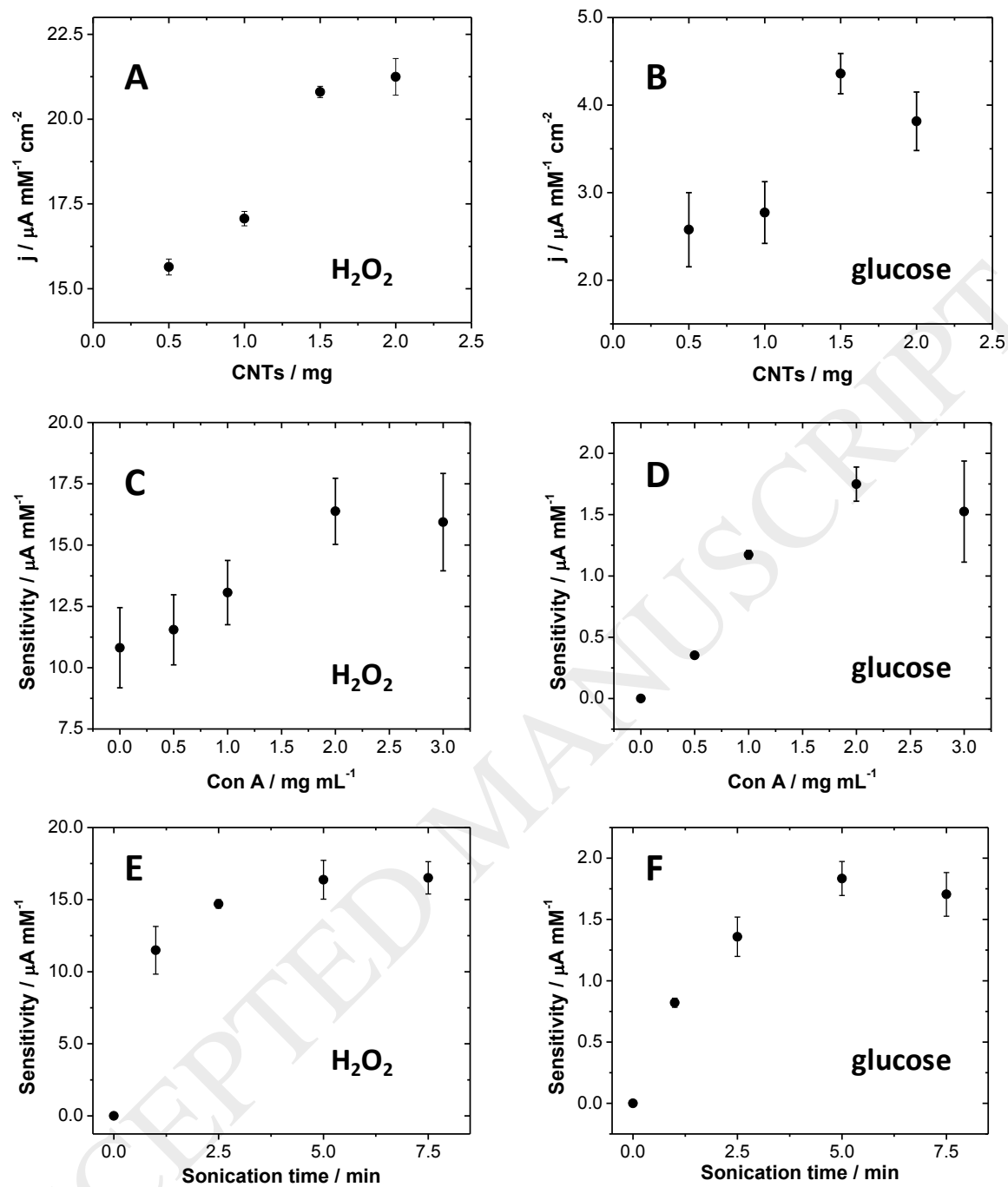


FIGURE 5- Rivas ET AL.

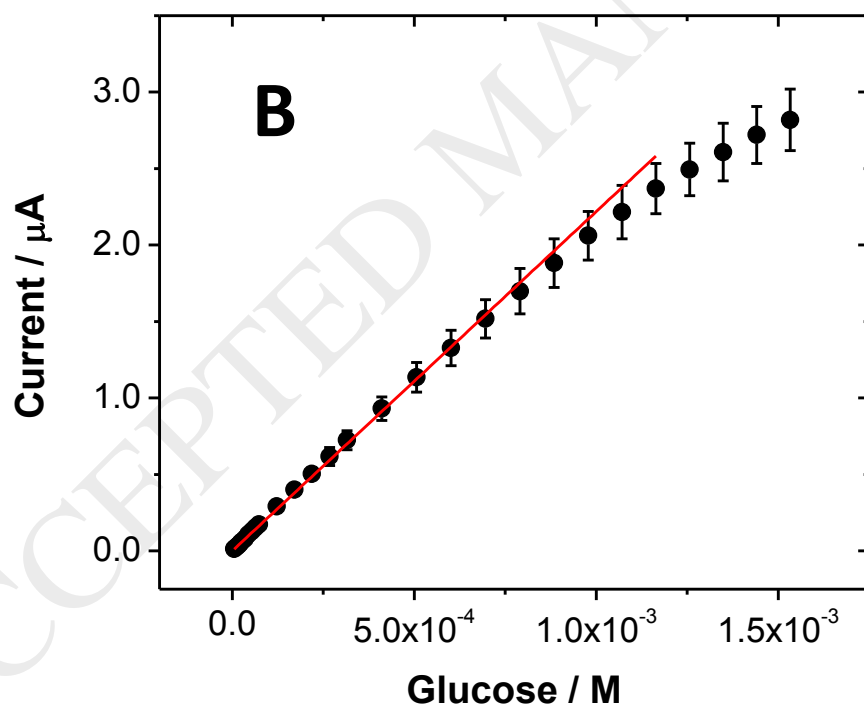
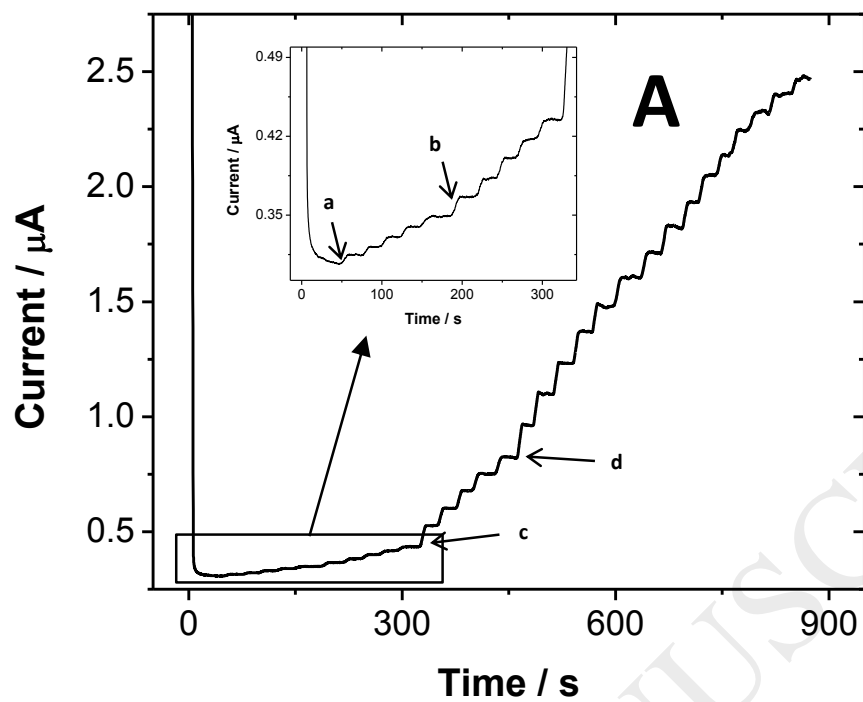


FIGURE 6- Rivas ET AL.

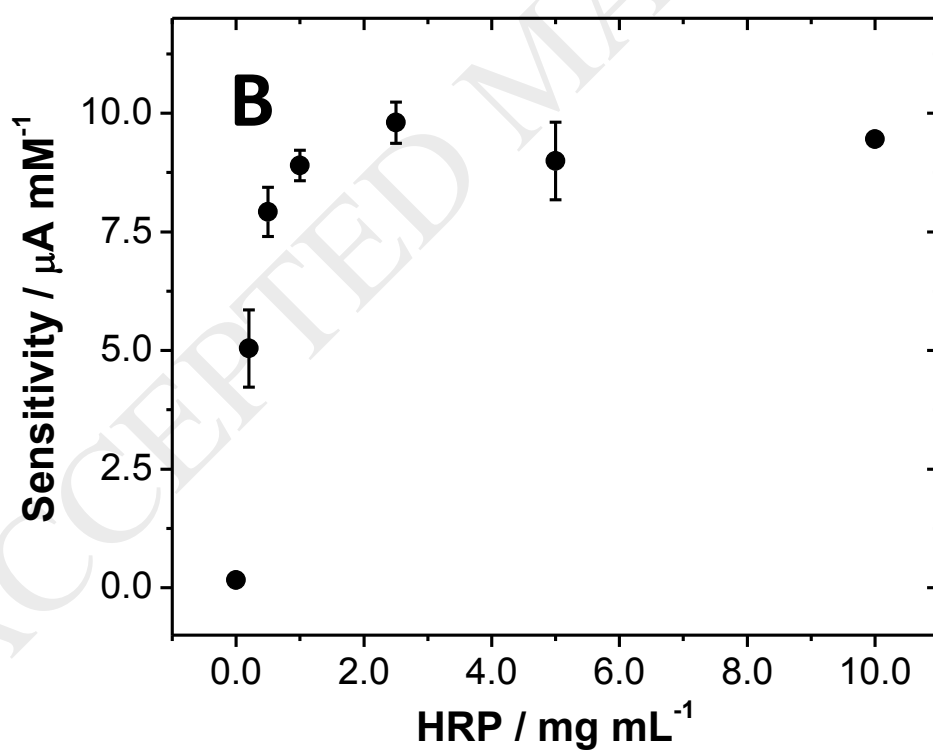
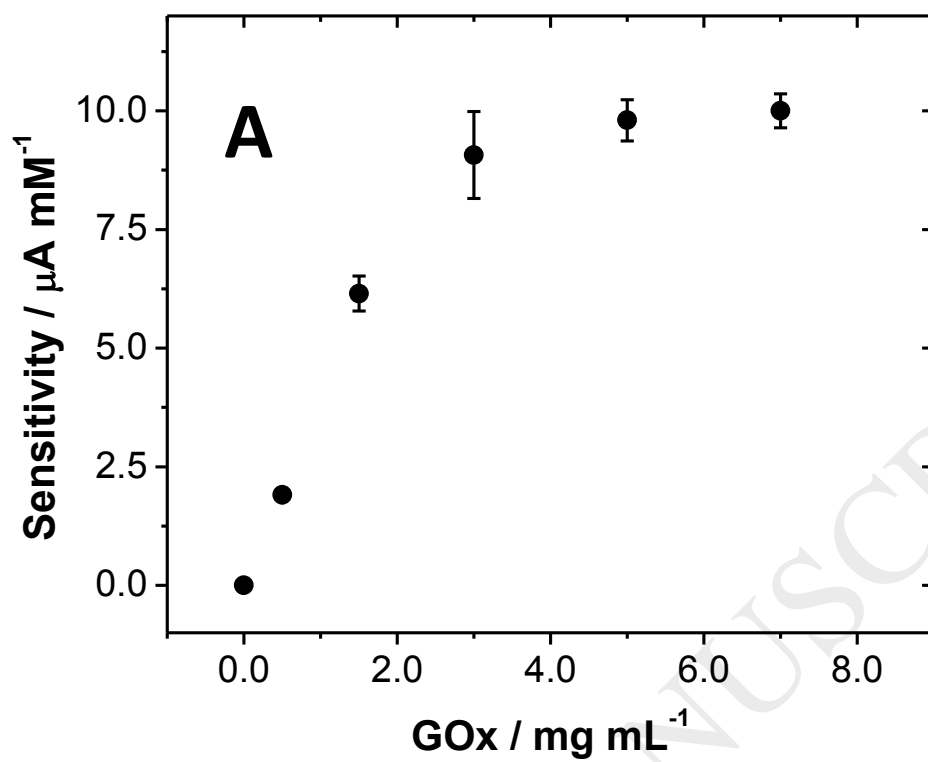


FIGURE 7- Rivas ET AL.

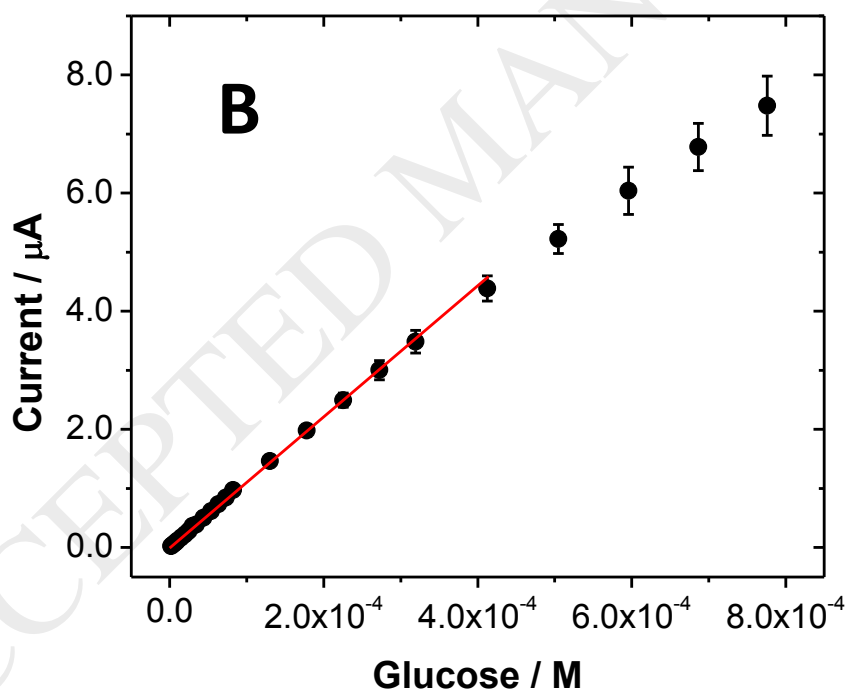
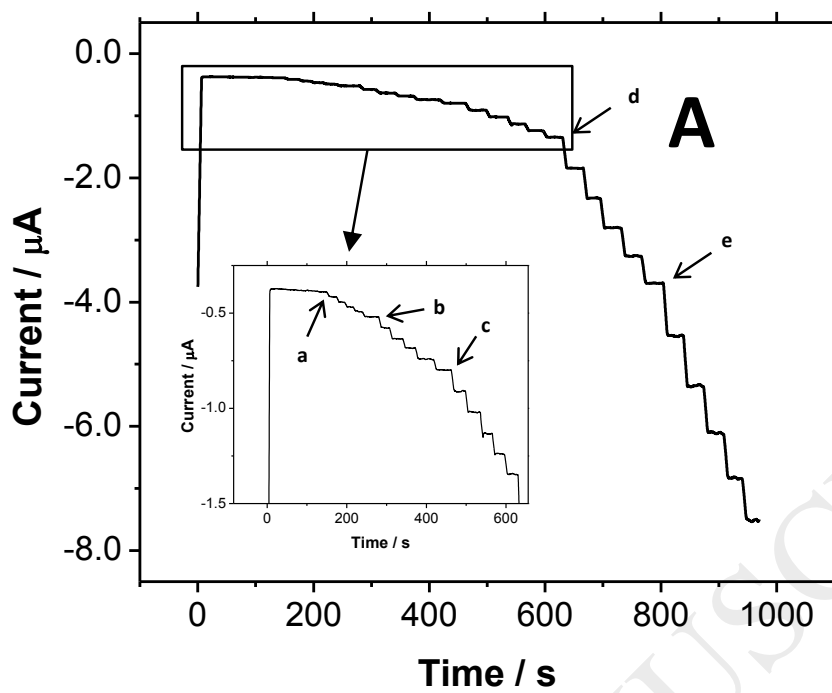


Table 1 – RIVAS ET AL.

ELECTROCHEMICAL PLATFORMS FOR GLUCOSE BIOSENSING					
Platform	Detection	Linear Range	Sensitivity	LOD	Ref.
GCE/(MWCNTs-Cyt c/GOx) ₂ /Naf	Amp. (-0.050 V)	(100 – 1000) μ M	0.096 μ A mM ⁻¹	8 μ M	[33]
GCE/MWCNTs-PEG/IL/GOx/Naf	Amp. (-0.270 V)	(20 – 950) μ M	--	0.2 μ M	[34]
GCE/rGO/pTB-HRP-GOx	Amp. (-0.100 V)	(80 – 1000) μ M	0.34 μ A mM ⁻¹	50 μ M	[35]
SPCE/ERGO/IL-CHO/GOx	Amp. (-0.450 V)	(50 – 2400) μ M	17.7 μ A mM ⁻¹ cm ⁻²	17 μ M	[36]
AuE/PEDOT-PSS/(CS-NGr-GOx) ₂	Amp. (-0.200 V)	(100 – 1400) μ M	237 μ A mM ⁻¹ cm ⁻²	41 μ M	[37]
GCE/AuNFs/GS-IL-AuNRs(sol-gel)/GOx/GA/Naf	Amp. (-0.200 V)	(1 – 764) μ M	0.06408 μ A mM ⁻¹	0.38 μ M	[38]
GCE/TCNFs-GOx	Amp. (-0.550 V)	(13 – 10500) μ M	628.82 μ A mM ⁻¹ cm ⁻²	3.7 μ M	[39]
GCE/KB/HRP-GOx-GA	Amp. (-0.100 V)	(5 – 1500) μ M	330 μ A mM ⁻¹ cm ⁻²	2 μ M	[40]
GCE/HNF-TiO ₂	Amp. (-0.450 V)	(2 – 3170) μ M	32.6 μ A mM ⁻¹ cm ⁻²	0.8 μ M	[41]
GCE/CaTiO ₃ NPs-GOx-CS	Amp. (-0.450 V)	(7 – 1490) μ M	14.1 μ A mM ⁻¹ cm ⁻²	2.3 μ M	[42]
Ti/Bi ₄ Ti ₃ O ₁₂ /GOx/NiONPs	Amp. (-0.442 V)	(20 – 3350) μ M	215 μ A mM ⁻¹ cm ⁻²	1.26 μ M	[43]
GCE/MWCNTs-ConA/GOx	Amp. (0.700 V)	(5 – 1200) μ M	(2.22 \pm 0.03) μ A mM ⁻¹	1.6 μ M	This work
GCE/MWCNTs-ConA/HRP-GOx	Amp. (-0.050 V)	(2 – 410) μ M	(11.5 \pm 0.4) μ A mM ⁻¹	0.31 μ M	

GCE: glassy carbon electrode; MWCNTs: multi-walled carbon nanotubes; Cyt c: cytochrome c; GOx: glucose oxidase; Naf: nafion; PEG: polyethylene glycol; IL: ionic liquid; rGO: reduced graphene oxide; pTB: poly(toluidine blue); HRP: horseradish peroxidase; SPCE: screen-printed carbon electrode; ERGO: electrochemically reduced graphene oxide; IL-CHO: aldehyde functionalized ionic liquid; AuE: gold electrode; PEDOT: poly(3,4-ethylenedioxythiophene); PSS: poly(styrene sulfonate); CS: chitosan; NGr: nitrogen doped graphene; AuNFs: gold nanoflowers; GS: graphene sheets; AuNRs: gold nanorods; GA: glutaraldehyde; TCNFs: titanium carbide-carbon nanofibers; KB: Ketjen Black; HNF: hollow nanofibers; CaTiO₃NPs: perovskite-type calcium titanate nanoparticles; NiONPs: nickel oxide nanoparticles.